JIPB Journal of Integrative Plant Biology

Research Article
https://doi.org/10.1111/jipb.13057

# Abscisic acid signaling negatively regulates nitrate uptake via phosphorylation of NRT1.1 by SnRK2s in *Arabidopsis*

Hang Su[1†], Tian Wang[1†], Chuanfeng Ju[1†], Jinping Deng[2], Tianqi Zhang[1], Mengjiao Li[3], Hui Tian[3] and Cun Wang[1*]

1. State Key Laboratory of Crop Stress Biology for Arid Areas and College of Life Sciences, Northwest A&F University, Yangling 712100, China
2. State Key Laboratory of Plant Physiology and Biochemistry, College of Biological Sciences, China Agricultural University, Beijing 100193, China
3. College of Natural Resources and Environment, Northwest A&F University, Yangling 712100, China
†These authors contributed equally to this work.
*Correspondence: Cun Wang (cunwang@nwafu.edu.cn)

Hang Su

Cun Wang

## ABSTRACT

Nitrogen (N) is a limiting nutrient for plant growth and productivity. The phytohormone abscisic acid (ABA) has been suggested to play a vital role in nitrate uptake in fluctuating N environments. However, the molecular mechanisms underlying the involvement of ABA in N deficiency responses are largely unknown. In this study, we demonstrated that ABA signaling components, particularly the three subclass III SUCROSE NON-FERMENTING1 (SNF1)-RELATED PROTEIN KINASE 2S (SnRK2) proteins, function in root foraging and uptake of nitrate under N deficiency in *Arabidopsis thaliana*. The *snrk2.2snrk2.3snrk2.6* triple mutant grew a longer primary root and had a higher rate of nitrate influx and accumulation compared with wild-type plants under nitrate deficiency. Strikingly, SnRK2.2/2.3/2.6 proteins interacted with and phosphorylated the nitrate transceptor NITRATE TRANSPORTER1.1 (NRT1.1) *in vitro* and *in vivo*. The phosphorylation of NRT1.1 by SnRK2s resulted in a significant decrease of nitrate uptake and impairment of root growth. Moreover, we identified NRT1.1$^{Ser585}$ as a previously unknown functional site: the phosphomimetic NRT1.1$^{S585D}$ was impaired in both low- and high-affinity transport activities. Taken together, our findings provide new insight into how plants fine-tune growth via ABA signaling under N deficiency.

Keywords: abscisic acid, nitrogen deficiency, NRT1.1, SnRK2.2/2.3/2.6

**Su, H., Wang, T., Ju, C., Deng, J., Zhang, T., Li, M., Tian, H., and Wang, C.** (2021). Abscisic acid signaling negatively regulates nitrate uptake via phosphorylation of NRT1.1 by SnRK2s in *Arabidopsis*. J. Integr. Plant Biol. **63:** 597–610.

## INTRODUCTION

Nitrogen (N) is a primary macronutrient for plants and a limiting factor in heterogeneous natural soils and agroecosystems. Since the nitrate supply in the soil is often insufficient to sustain optimal plant growth and development in agricultural production systems, farmers have to fertilize with large amounts of N to enable maximal crop yield, and the use of synthetic N has increased remarkably. However, crops use only 30%–50% of the N applied (Miller and Cramer, 2004). The remaining N is lost to runoff or leaching and pollutes nearby waterways. To reduce the overuse of N fertilizer and alleviate environmental pollution, improving N-use efficiency (NUE) is a global goal for crop breeders (Oldroyd and Leyser, 2020). In addition to acting as a N source, nitrate serves as a signal molecule that modulates numerous processes, including root architecture, shoot development, seed germination, flowering, and circadian rhythms (O'Brien et al., 2016; Lin and Tsay, 2017). Short-term, local nitrate signaling is integrated with long-term, systematic nitrate signaling to

orchestrate root growth in response to fluctuating N environments (Ohkubo et al., 2017; Osugi et al., 2017).

Plants actively take up nitrate from the environment using a proton/nitrate-coupled mechanism (Wang et al., 2018). Nitrate is primarily absorbed into roots via nitrate transporters from NITRATE TRANSPORTER1 (NRT1)/PEPTIDE TRANSPORTER (PTR) (NPF) and NRT2 families (Tsay, 1993; Li et al., 2007; Kiba et al., 2012; Lezhneva et al., 2014). There are 53 *NRT1* genes and seven *NRT2* genes in the *Arabidopsis thaliana* genome. Among these, NRT1.1/NPF6.3/CHLORATE RESISTANT 1 (CHL1) was the first nitrate transporter identified in plants and exhibits a characteristic dual affinity. AtNRT1.1 displays auxin transport activity and mediates nitrate-modulated root development, indicating that it has the capacity to transport multiple substrates (Krouk et al., 2010). Indeed, the deletion of NRT1.1 impairs nitrate acquisition and translocation, as well as auxin transport (Tsay, 1993; Nien-Chen Huang et al., 1996; Krouk et al., 2010; Leran et al., 2013). Further study demonstrated that NRT1.1$^{Thr101}$ is a crucial phosphorylation site targeted by calcineurin B-like proteins-interacting protein kinase (CIPK23) to regulate nitrate and auxin transport activity, nitrate signaling, and the inhibition of lateral root elongation under N deficiency (Tsay, 2003; Ho et al., 2009; Bouguyon et al., 2015; Zhang et al., 2019). The presence of nitrate can increase the transcription of *AtNRT1.1* and the accumulation of messenger RNA (mRNA) in lateral root primordia, but represses its protein accumulation with a concomitant increase in the accumulation of auxin to promote lateral root elongation (Bouguyon et al., 2016). Notably, transcription factors such as TEOSINTE BRANCHED 1/CYCLOIDEA/PROLIFERATING CELL FACTOR 1–20 (TCP20) and NITRATE REGULATORY GENE2 (NRG2) can bind directly to the promoter of *NRT1.1* to positively regulate its expression. In addition, LATERAL BOUNDARY DOMAIN37 (LBD37) and LBD38 act as repressors of *NRT1.1* (Rubin et al., 2009; Guan et al., 2014; Xu et al., 2016). However, the molecular mechanisms that underlie nitrate acquisition and signaling are still largely unknown.

Abscisic acid (ABA) regulates diverse cellular and molecular processes during plant development and in response to abiotic stresses (Xu et al., 2019; Chen et al., 2020; Qi et al., 2020). Abscisic acid is recognized by receptors including PYRABACTIN RESISTANCE/PYRABACTIN RESISTANCE-LIKE/REGULATORY COMPONENT OF ABSCISIC ACID RECEPTOR (PYR/PYL/RCAR) family proteins, which combine with clade A PROTEIN PHOSPHATASES OF TYPE 2C (PP2C) to function as coreceptors for ABA (Fujita et al., 2009; Umezawa et al., 2009; Gonzalez-Guzman et al., 2012). In the presence of ABA, the PYR proteins inhibit the activity of PP2Cs and de-repress the catalytic functions of a small subfamily of SUCROSE NON-FERMENTING1 (SNF1)-RELATED PROTEIN KINASE 2s (SnRK2s). Three subclass III SnRK2 protein kinases, SnRK2.2/SRK2D, SnRK2.3/SRK2I, and SnRK2.6/SRK2E/OPEN STOMATA1 (OST1), are strongly activated by ABA and consequently phosphorylate downstream effectors, such as the slow-sustained anion channel1 (SLAC1), the potassium channel $K^+$ *Arabidopsis thaliana* 1 (KAT1), the transcription factors ABA-insensitive 5 (ABI5), myeloblastosis (MYB), and *NAM*, *ATAF*, *CUC* genes (*NAC*), and reduced form of oxidized nicotinamide adenine dinucleotide phosphate (NADPH) oxidase, thereby activating stress responses (Geiger et al., 2009; Sato et al., 2009; Sirichandra et al., 2009; Nuruzzaman et al., 2013; Lee and Seo, 2019). Abscisic acid signaling has been reported to play essential roles in root foraging by ABI2/PP2C under mild N deficiency, and ABA regulates the expression of *NRT2/NAR* under conditions of limited nitrate (Leran et al., 2015; Wang et al., 2020). However, the molecular mechanisms connecting ABA to nitrate deficiency signaling are still largely unclear.

In this study, we report that SnRK2.2, SnRK 2.3, and SnRK 2.6 are key regulators of NRT1.1. SnRK2.2/2.3/2.6 physically interact with and phosphorylate NRT1.1. The phosphorylation of NRT1.1 by SnRK2s resulted in decreased nitrate uptake and impaired root growth. Additionally, we identified Ser585 as a functional site in NRT1.1 important for its nitrate transport activity. In conclusion, our findings support a model in which SnRK2.2/2.3/2.6 serve as core intersection points between ABA signaling and nitrate deficiency responses.

## RESULTS

### Abscisic acid signaling modulates root growth under nitrogen deficiency

To identify the novel components that mediate plant adaptation to N starvation, we performed a reverse genetic approach, screening a variety of *Arabidopsis* mutants that differed in their signal transduction in response to N deficiency. The elongation of both primary and lateral roots, as well as the emergence of new lateral roots, were inhibited following exposure to a low concentration of external N. Compared with rigorous N limitation, mild N deficiency stimulates the emergence of lateral roots and particularly the elongation of primary and lateral roots (Gruber et al., 2013; Giehl and von Wiren, 2014). Thus, we focused on the phenotypes of primary and lateral roots under N deficiency. Four-d-old homogenous seedlings germinated on 1/2 Murashige and Skoog (MS) medium containing 20 mmol/L $NO_3^-$ were transferred to MS medium containing 0 or 0.05 mmol/L $KNO_3$ for 7 additional d. We observed that the ABA-deficient mutant *aba2-1* grew longer primary roots and had a higher lateral root density compared with the wild type (WT) under N deficiency (Figure 1A–C). We then examined the phenotypes of the quadruple ABA receptor mutant *pyr1pyl1pyl2pyl4* and the *PP2Cs* quadruple mutant *abi1-2abi2-2hab1-1pp2ca-1* to investigate whether ABA is involved in the response to N deficiency. Like the *aba2-1* mutant, the *pyr1pyl1pyl2pyl4* mutant displayed longer primary roots and a higher lateral root density compared with the WT under N deficiency (Figure 1A–C). By contrast, the

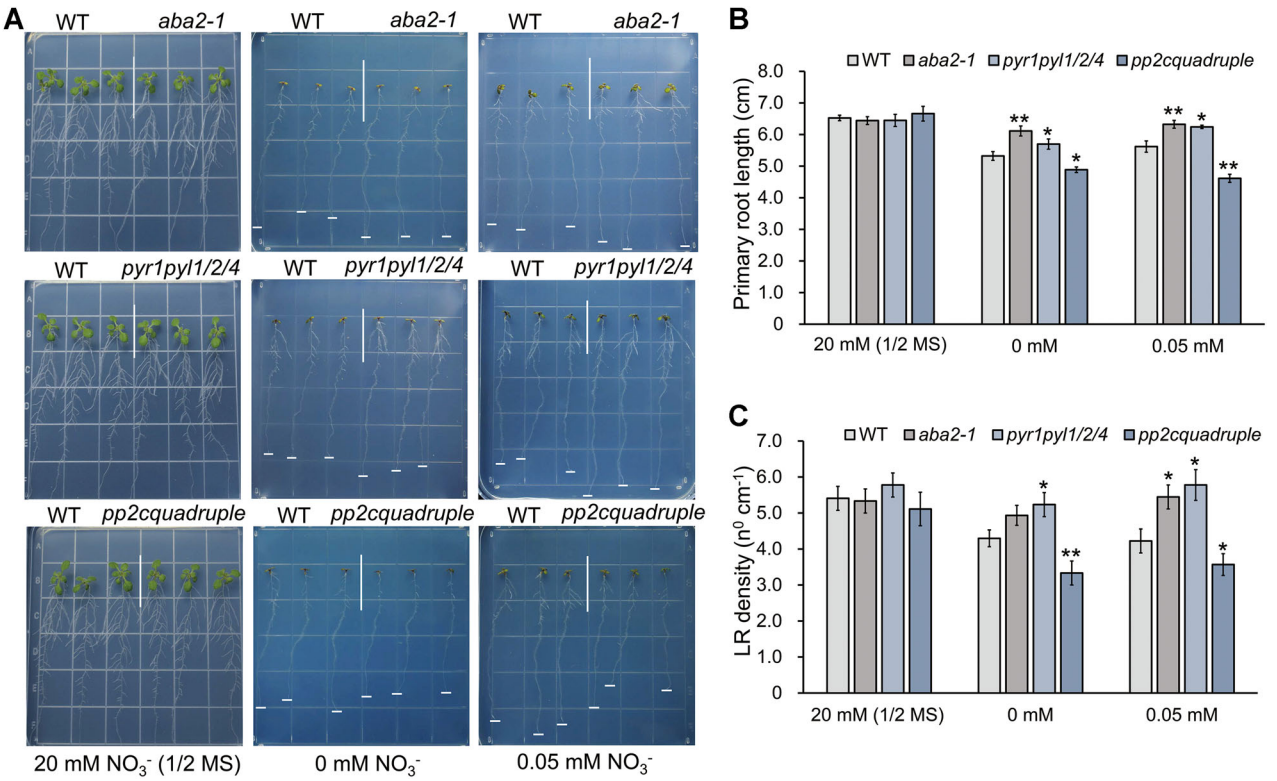


**Figure 1. Phenotypic analysis of abscisic acid (ABA) signaling mutants under nitrogen deficiency**

(**A**) Phenotypic analysis of the tested mutants under 0, 0.05, and 20 mmol/L $NO_3^-$ (1/2 Murashige and Skoog (MS)). (**B**) Primary root length of the tested mutants under the different nitrate treatments ($n = 24$). (**C**) Lateral root density under the different nitrate treatments ($n = 24$). Error bars represent means ± *SE*. Asterisks indicate statistically significant differences according to honestly significant difference (HSD) test (*$P < 0.05$, **$P < 0.01$).

*abi1-2abi2-2hab1-1pp2ca-1* mutant grew shorter primary roots and had a lower root density compared with the WT under N deficiency (Figure 1A–C). None of the mutants showed differences in the length of their primary roots and lateral root density compared to the WT when grown on 1/2 MS medium. Taken together, these results demonstrate that ABA signaling plays a negative role in the response to N deficiency in *Arabidopsis*.

## SnRK2.2/2.3/2.6 regulate root growth and alter nitrate uptake under N deficiency

There are 10 SnRK2 proteins in *Arabidopsis*, among which SnRK2.2, SnRK2.3, and SnRK2.6/OST1 are core kinases and function redundantly in ABA signaling (Fujii and Zhu, 2009; Fujita et al., 2009). For this reason, we tested *snrk2.6*, *snrk2.2snrk2.3*, and *snrk2.2snrk2.3snrk2.6* mutants under N deficiency. The *snrk2.6/ost1* and *snrk2.2snrk2.3* mutants grew a slightly longer primary root than the WT under N deficiency (Figure S1), and the *snrk2.2snrk2.3snrk2.6* mutant grew a significantly longer primary root than the WT, while there were no differences in their lateral root densities (Figure 2A). Based on all these results, we conclude that SnRK2.2/2.3/2.6 function redundantly in response to N deficiency in *Arabidopsis*. To further explore SnRK2.2, SnRK2.3, and SnRK2.6/OST1 participation in the N deficiency response, we examined transgenic plants overexpressing (OE) *SnRK2.2*, *SnRK2.3*, or *SnRK2.6/OST1* (Feng et al., 2014) upon N deficiency treatment; however, the *OE* lines did not differ significantly from the WT in primary root length and lateral root density (Figure S2).

To investigate whether the longer root of the *snrk2.2snrk2.3snrk2.6* mutant was due to elevated N uptake, we analyzed the influx of $NO_3^-$ by measuring $NO_3^-$ flux at the root surface. First, 4-d-old homogenous seedlings germinated on 1/2 MS medium were transferred to N-free medium supplemented with 0.01 mmol/L $NO_3^-$. After treatment for 4 d, nitrate flux at the seedling root surface was analyzed using the non-invasive high-resolution scanning ion-selective electrode technique (SIET). We used the NRT1.1 deletion mutant *chl1-5* as our experimental control, in which nitrate uptake is abolished (Ho et al., 2009). The *snrk2.2snrk2.3snrk2.6* mutant showed a substantially higher rate of nitrate influx than the WT under N deficiency, while the *chl1-5* mutant exhibited a much lower rate of nitrate influx (Figure 2C, D). To investigate whether ABA affects nitrate influx under N deficiency, we performed the nitrate influx assay in WT, *chl1-5*, and *snrk2.2snrk2.3snrk2.6* seedlings treated with 10 μmol/L ABA. Abscisic acid suppressed nitrate influx in the WT and the *chl1-5* mutant, but not in the *snrk2.2snrk2.3snrk2.6* mutant (Figure 2C, D). These results indicated that ABA negatively regulates nitrate acquisition via SnRK2.2/2.3/2.6 under N deficiency.

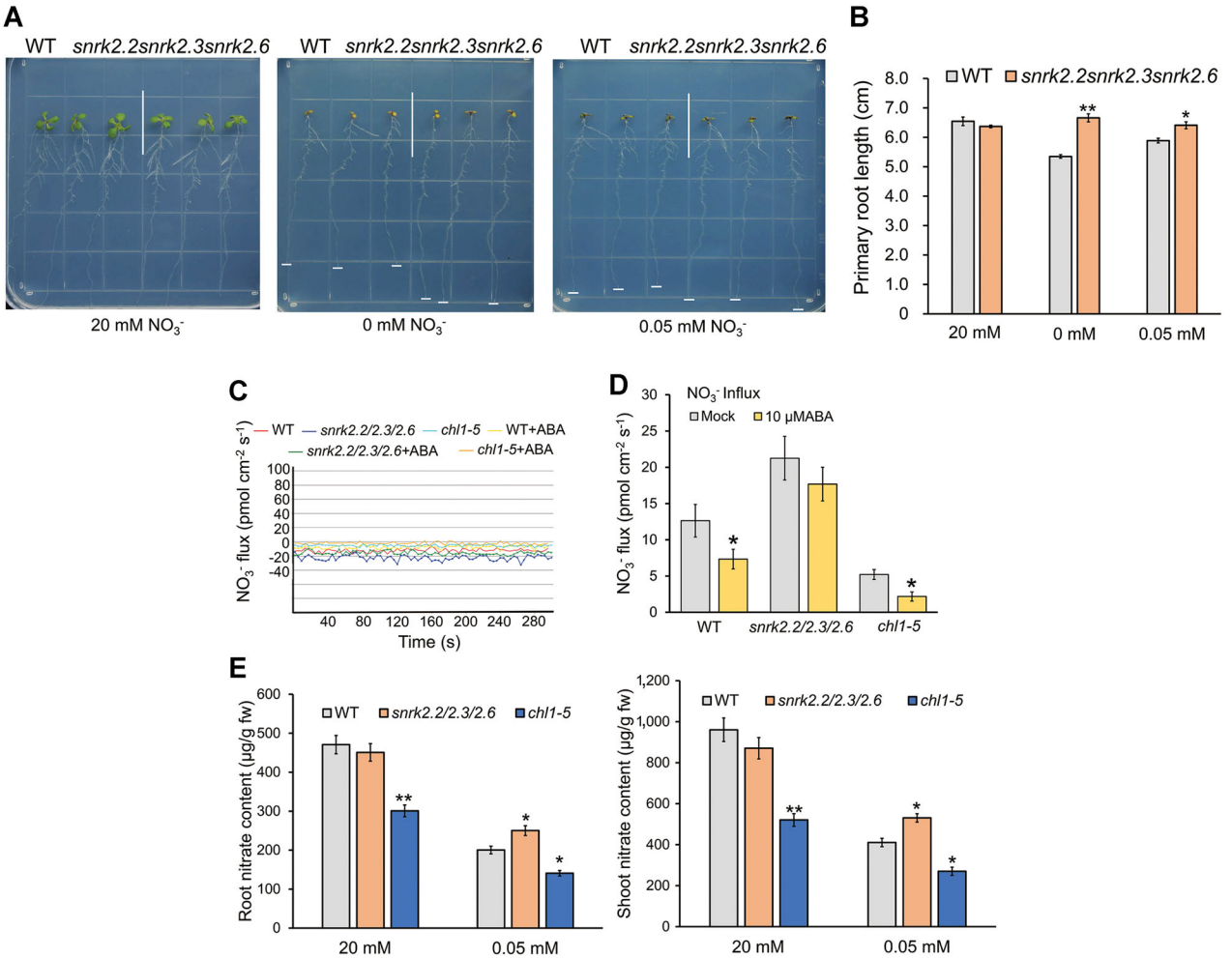


**Figure 2. SnRK2s regulate root growth and nitrate uptake under nitrogen deficiency**

(**A**) Phenotype of the *snrk2.2snrk2.3snrk2.6* triple mutant under 0, 0.05, and 20 mmol/L $NO_3^-$. (**B**) Primary root length of the *snrk2.2snrk2.3snrk2.6* triple mutant under the different nitrate treatments ($n = 24$). Error bars represent means ± *SE*. Asterisks indicate statistically significant differences according to honestly significant difference (HSD) test (*$P < 0.05$, **$P < 0.01$). (**C**) Nitrate influx rate at the root tip surface ($n = 12$). (**D**) N-influx measurement in the wild type (WT) and the tested mutants. (**E**) Nitrate content in roots and shoots. Error bars represent means ± *SE*. Asterisks indicate statistically significant differences according to Student's *t*-test (*$P < 0.05$, **$P < 0.01$).

Furthermore, we tested the contents of nitrate in the *snrk2.2snrk2.3snrk2.6* triple mutant and the *chl1-5* mutant grown in 1/2 N-free MS medium supplemented with 0.05 mmol/L $NO_3^-$. The accumulation of nitrate in both the roots and shoots of the *snrk2.2snrk2.3snrk2.6* triple mutant under N deficiency was significantly higher than that of the WT (Figure 2E). These results indicated that ABA negatively regulates nitrate acquisition via SnRK2.2/2.3/2.6 under N deficiency.

## SnRK2s interact with NRT1.1 *in vitro* and *in vivo*

Considering that SnRK2.2/2.3/2.6 appear to participate in the regulation of nitrate acquisition, we hypothesized that SnRK2.2/2.3/2.6 may interact directly with nitrate transporters. To test this hypothesis, we used a dual-membrane screening system of a yeast two-hybrid assay (Y2H) to screen potential nitrate transporter candidates that might interact with SnRK2.2/2.3/2.6, such as NRT1.1, NRT2.1, NRT2.2, NRT2.4, and NRT2.5. Notably, only the yeast cells transfected with SnRK2.6/OST1 and NRT1.1 grew well on synthetic dropout medium that lacked threonine, leucine, histidine, and alanine, and even on selection medium supplemented with 3-amino-1,2,4-triazole (3-AT), while the control cells could not grow under these conditions. These results indicated that SnRK2.6/OST1 physically and specifically interacts with NRT1.1, while SnRK2.2 and SnRK2.3 might not (Figure 3A).

To validate the protein interaction results obtained from the Y2H assay, we performed bimolecular fluorescence complementation (BiFC) in the epidermal cells of *Nicotiana benthamiana* leaves. NRT1.1 interacted with all the subgroup III SnRK2s in the plasma membrane, whereas no significant signals were observed in controls that lacked NRT1.1 or SnRK2s (Figure 3B). Notably, SnRK2.6/OST1 interacted

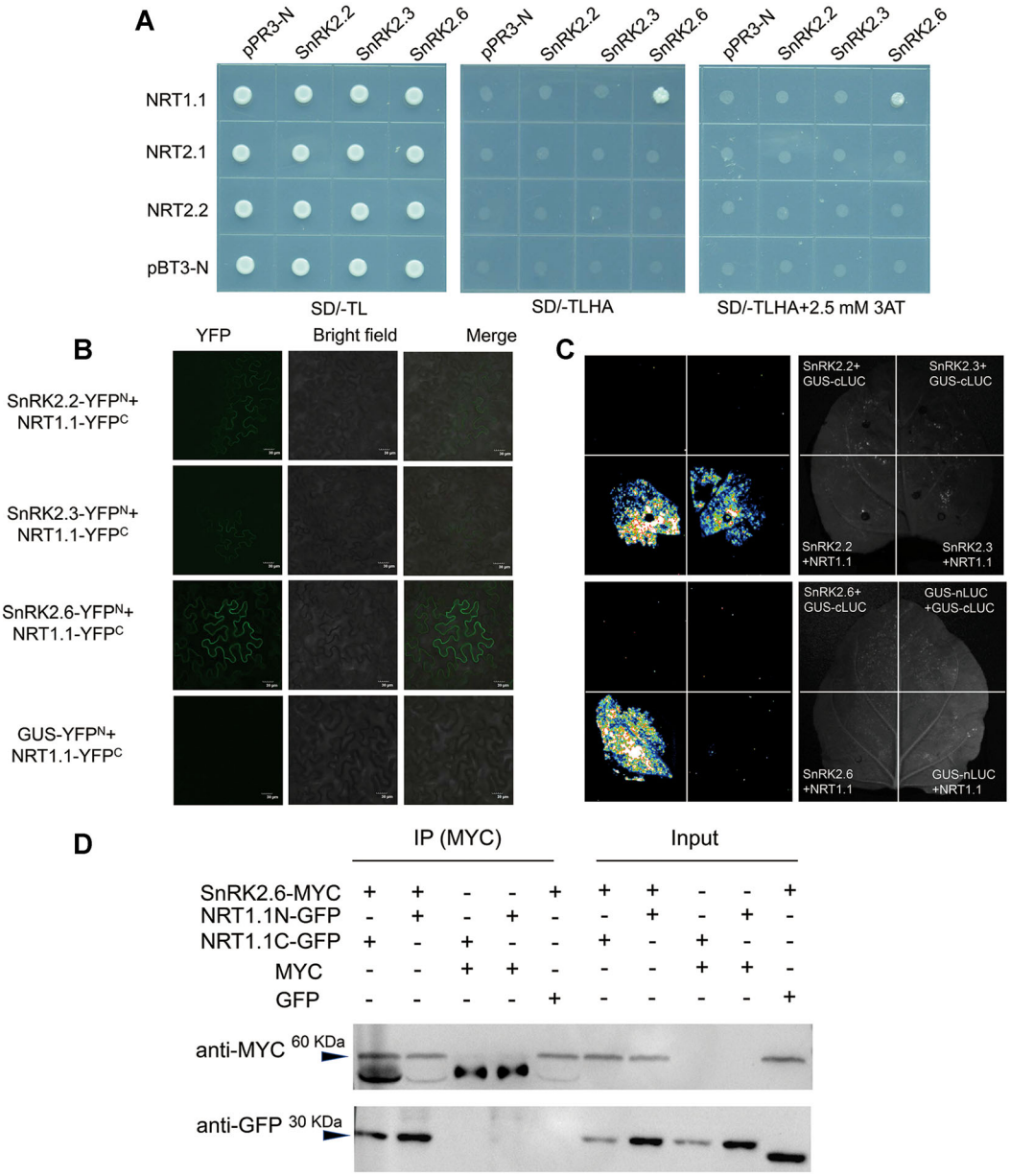


**Figure 3. SnRK2s physically interact with NRT1.1**

(**A**) Yeast-based split ubiquitin system assays of SnRK2.2/2.3/2.6 with NRT1.1. *pBT3-N*, empty bait vector; *pPR3-N*, empty prey vector; SD/–TL, synthetic defined (SD) medium lacking threonine and leucine; SD/–TLHA, SD medium lacking threonine, leucine, histidine, and alanine; 3-AT, 3-amino-1,2,4-triazole. (**B**) Bimolecular fluorescence complementation analyses of SnRK2.2/2.3/2.6 with NRT1.1. N- and C-terminal fragments of yellow fluorescent protein (YFP) were fused to SnRK2s and NRT1.1, respectively. Reconstituted fluorescent YFP signals (left column) and bright field images (middle column) were merged (right column). (**C**) Luciferase complementation imaging analyses of SnRK2.2/2.3/2.6-nLUC with cLUC-NRT1.1 in *Nicotiana benthamiana* leaves. (**D**) Co-immunoprecipitation assays of SnRK2.6/OST1-MYC with NRT1.1 N and NRT1.1 C terminal-GFP (green fluorescent protein) in *N. benthamiana* leaves.

more strongly with NRT1.1 compared with SnRK2.2 and SnRK2.3. Furthermore, we conducted a split-luciferase complementation (Split-LUC) assay in *N. benthamiana* leaves. The co-expression of SnRK2.2-, SnRK2.3-, and SnRK2.6/OST1-nLUC with cLUC-NRT1.1 reconstituted the activity of luciferase (Figure 3C). By contrast, the co-expression of nLUC/cLUC, nLUC/cLUC-NRT1.1, or subgroup III SnRK2s-nLUC/cLUC resulted in only background luciferase signals. Similarly, the co-expression of SnRK2.6/OST1-nLUC/cLUC-NRT1.1 produced stronger luciferase activity than those of SnRK2.2-nLUC/cLUC-NRT1.1 and SnRK2.3-nLUC/cLUC-NRT1.1, confirming the results from the BiFC assays.

We next performed co-immunoprecipitation (Co-IP) assays in *N. benthamiana* leaves to verify this protein interaction. The expression of full-length NRT1.1 protein was unsatisfactory in our system; crystal structure and putative membrane topology analyses of NRT1.1 showed that it has a 28-amino-acid-long

N-terminal and a 27-amino-acid-long C-terminal cytoplasmic segment (NT and CT), which is highly conserved among its plant orthologs. The cytoplasmic segments provide a potential protein-docking site, which indicated a potential role in recruiting kinases and phosphatases (Sun et al., 2014). Thus, we transiently co-expressed green fluorescent protein (GFP)-tagged NRT1.1 NT or NRT1.1 CT with MYC-tagged SnRK2.6/OST1 in *N. benthamiana*. A Co-IP assay using these materials revealed that SnRK2.6/OST1 interacted with both NRT1.1 NT and NRT1.1 CT (Figure 3D). In conclusion, these results demonstrate that SnRK2s interact with NRT1.1 *in vitro* and *in vivo*.

## SnRK2s phosphorylate and inhibit NRT1.1, and NRT1.1$^{Ser585}$ is the functional phosphorylation site

SnRK2s can phosphorylate a variety of transcription factors and transporters to relay ABA signals (Chen et al., 2020). In our experiments, SnRK2.6/OST1 interacted more strongly with NRT1.1 than did SnRK2.2/2.3, and SnRK2.2/2.3 were previously shown to have low kinase activity (Feng et al., 2014). Accordingly, we chose SnRK2.6/OST1 for *in vitro* kinase assays to test for phosphorylation of NRT1.1. As NRT1.1 has 12 transmembrane domains, we were unable to purify the full-length protein. Therefore, NRT1.1 NT- and NRT1.1 CT-GST fused proteins and SnRK2.6/OST1-MBP fused protein purified from *Escherichia coli* were used in the kinase assays. Both NRT1.1 NT and NRT1.1 CT were phosphorylated after incubation with the purified SnRK2.6/OST1 fusion protein (Figure 4B).

To identify the phosphorylation sites of NRT1.1 by SnRK2.6/OST1, we analyzed all possible phosphorylation sites of both N-terminal and C-terminal cytoplasmic segments of NRT1.1, including Ser2, Thr6, Ser8, Thr28, and Ser585 (Figure 4A). We substituted these sites with Ala to mimic non-phosphorylation. The phosphorylation of NRT1.1 NT$^{S2A}$, NRT1.1 NT$^{T6A}$, and NRT1.1 NT$^{T28A}$ were still evident after coincubation with SnRK2.6/OST1-MBP, whereas there was almost no phosphorylation signal on NRT1.1 NT$^{S8A}$ and NRT1.1 CT$^{S585A}$ (Figure 4B). Notably, Ser585 was very recently predicted to be a functional phosphorylation site of NRT1.1 based on a mass-spectrometry-based draft of the *Arabidopsis* proteome (Mergner et al., 2020). Taken together, our results demonstrate that SnRK2.6/OST1 phosphorylates both the NT and CT cytoplasmic segments of NRT1.1, and Ser8 and Ser585 are key phosphorylation sites *in vitro*.

To determine the biological function of phosphorylation of NRT1.1 by SnRK2.6/OST1, the nitrate uptake activity of NRT1.1 was examined in *Xenopus* oocytes. *NRT1.1* and *SnRK2.6/OST1* complementary RNAs (cRNAs) were co-injected into oocytes, and the abundance of $^{15}NO_3^-$ was measured after 2 d incubation in either 10 or 0.5 mmol/L $^{15}$N-nitrate. The oocytes injected with *NRT1.1* alone exhibited distinct nitrate transport activity at both nitrate levels compared with the oocytes that were injected with $H_2O$ (negative control) (Ho et al., 2009), whereas those injected with *SnRK2.6/OST1* alone showed no observable activity to transport nitrate. When the oocytes were co-injected with *NRT1.1* and *SnRK2.6/OST1* cRNAs, the uptake of nitrate was remarkably attenuated compared with cells that were injected only with *NRT1.1*, at both nitrate levels, demonstrating that SnRK2.6/OST1 inhibits both low- and high-affinity nitrate uptake activities of NRT1.1 (Figure 4C).

We then mutated the key amino acids NRT1.1$^{Ser8}$ and NRT1.1$^{Ser585}$ to Asp (mimicking phosphorylation). Nitrate uptake assays using 10 and 0.5 mmol/L nitrate were conducted to identify the functional phosphorylation sites of NRT1.1. The measurement of nitrate uptake in the 10 mmol/L nitrate treatment showed that the oocytes injected with *NRT1.1*$^{S8D}$ transported nitrate normally, whereas oocytes injected with *NRT1.1*$^{S585D}$ showed reduced nitrate uptake activity (Figure 4C). The uptake of nitrate in the 0.5 mmol/L nitrate treatment was similar to the results of the 10 mmol/L treatment (Figure 4D). These data showed that both the low- and high-affinity nitrate uptake activities of NRT1.1$^{S585D}$ were reduced. Together, these results suggest that phosphorylation by SnRK2.6/OST1 inhibits the nitrate transport activity of NRT1.1, and Ser585 could be a functional site.

To investigate whether SnRK2s phosphorylate NRT1.1$^{Ser585}$ *in vivo*, we performed an in-gel kinase assay. Total protein prepared from 10-d-old WT and *snrk2.2snrk2.3snrk2.6* plants with or without 50 μmol/L ABA were separated by sodium dodecyl sulfate – polyacrylamide get electrophoresis (SDS-PAGE) gel containing 0.1 mg/mL glutathione S-transferase (GST)-NRT1.1-C substrate. Both SnRK2.6/OST1 and SnRK2.2/2.3 could phosphorylate NRT1.1-C upon ABA treatment in the WT, while no phosphorylation signals were detected in the *snrk2.2snrk2.3snrk2.6* mutant (Figure 4E). Taken together, these results indicate that SnRK2s phosphorylate NRT1.1 in an ABA-dependent manner.

To further elucidate whether NRT1.1$^{Ser585}$ is the functional phosphorylation site *in planta*, we introduced a WT *NRT1.1* coding region fragment that contained the S8A, S8D, S585D, or S585A mutation into the *chl1-5* mutant under its own promoter (Figure S5). The NRT1.1$^{S585D}$/*chl1-5* lines grew an obviously shorter primary root both under control and N-deficiency conditions compared with the WT, which was a similar phenotype to that of the *chl1-5* mutant (Figure 5A, C). By contrast, the NRT1.1/*chl1-5*, NRT1.1$^{S585A}$/*chl1-5*, NRT1.1$^{S8D}$/*chl1-5*, and NRT1.1$^{S8A}$/*chl1-5* transgenic lines displayed no significant differences compared with the WT (Figures 5B, C, S3). Furthermore, the NRT1.1$^{S585D}$/*chl1-5* lines showed a similar rate of nitrate influx to that of the *chl1-5* mutant, which was significantly lower than that in the WT, NRT1.1/*chl1-5*, and NRT1.1$^{S585A}$/*chl1-5* plants (Figure 5D, E). Collectively, these results confirmed that Ser585 of NRT1.1 is a crucial functional site of NRT1.1.

We wondered whether phosphorylation of NRT1.1 by SnRK2s affected its ABA responses; therefore, we subjected the NRT1.1$^{S585D}$/*chl1-5* and NRT1.1$^{S585A}$/*chl1-5* seedlings to ABA treatment and examined their phenotypes. Four-d-old seedlings germinated on 1/2 MS medium were transferred to

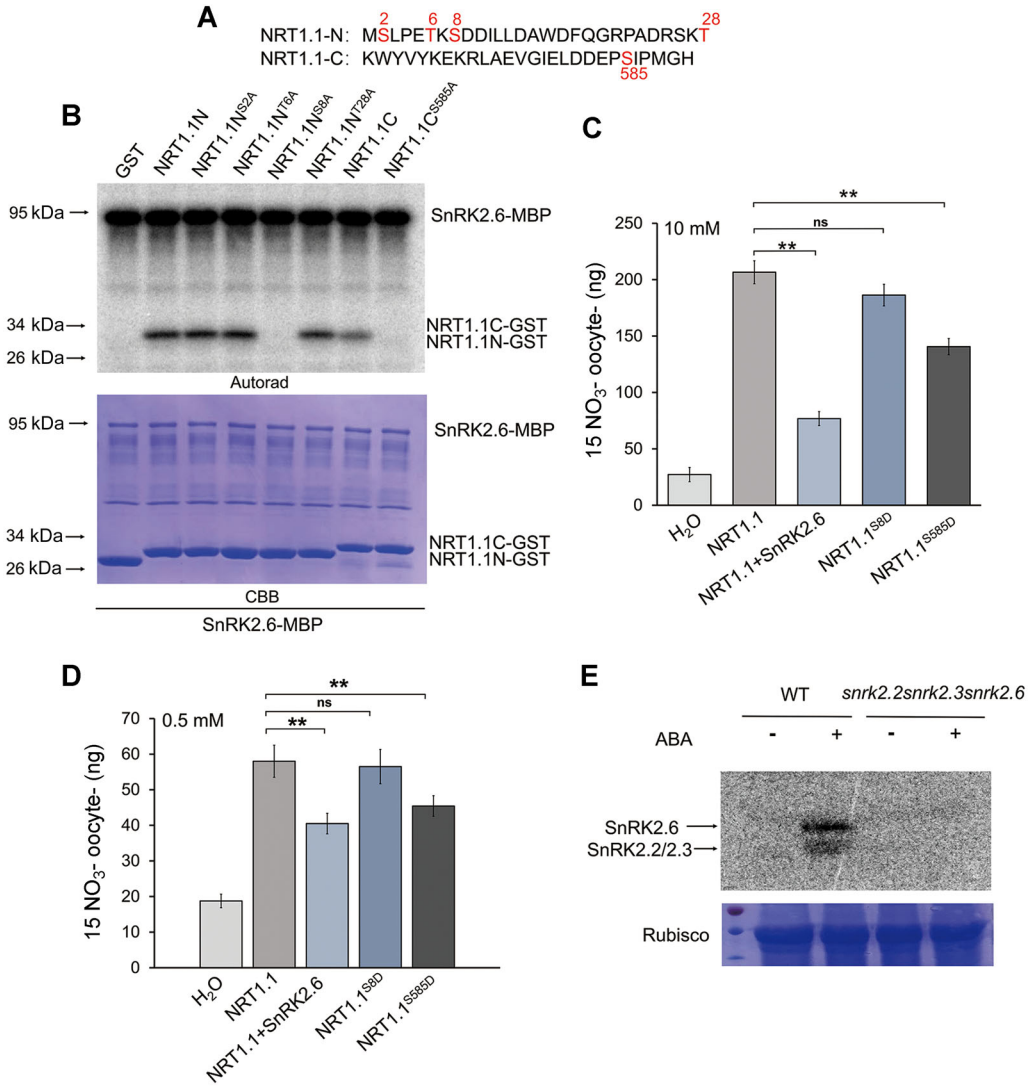


**Figure 4. SnRK2s phosphorylate NRT1.1 and inhibit its activity**

(**A**) Candidates for SnRK2.6/OST1 phosphorylation sites of NRT1.1N -and NRT1.1C terminals. (**B**) *In vitro* phosphorylation of NRT1.1 by SnRK2.6/OST1. glutathione S-transferase (GST)-NRT1.1 N, GST-NRT1.1N$^{S2A}$, GST-NRT1.1N$^{T6A}$, GST-NRT1.1N$^{S8A}$, GST-NRT1.1N$^{T28A}$, GST-NRT1.1 C, GST-NRT1.1C$^{S585A}$, and SnRK2.6/OST1-MBP were expressed in *Escherichia coli* BL21 and purified. [γ-$^{32}$P] adenosine triphosphate autoradiography was used to detect kinase activity of SnRK2.6/OST1. Coomassie blue staining was used to confirm these NRT1.1 N and NRT1.1 C proteins. Line 1 to line 8 show GST, GST-NRT1.1 N, GST-NRT1.1N$^{S2A}$, GST-NRT1.1N$^{T6A}$, GST-NRT1.1N$^{S8A}$, GST-NRT1.1N$^{T28A}$, GST-NRT1.1 C, and GST-NRT1.1C$^{S585A}$. (**C**) and (**D**) Nitrate transport activity of phosphorylated NRT1.1 by SnRK2.6/OST1 in *Xenopus* oocytes. Nitrate uptake assays in oocytes injected with cRNAs of *NRT1.1*, *NRT1.1*$^{S8D}$, and *NRT1.1*$^{S585D}$, or co-injected with *SnRK2.6/OST1* were conducted using 10 mmol/L $^{15}NO_3^-$ (**C**) or 0.5 mmol/L $^{15}NO_3^-$ (**D**) by continuous-flow mass spectrometry. Values are means ± *SE* ($n = 8$–10). Asterisks indicate statistically significant differences according to Student's *t*-test (*$P < 0.05$, **$P < 0.01$, ns, not significant). (**E**) In-gel kinase assay of SnRK2s with NRT1.1. Total protein prepared from 10-d-old wild type (WT) and *snrk2.2snrk2.3snrk2.6* plants was separated by sodium dodecyl sulfate – polyacrylamide get electrophoresis gel containing 0.1 mg/mL GST-NRT1.1 substrate. Plants treated with 50 μmol/L abscisic acid (ABA) were used as a control. Rubisco is shown in the bottom.

1/2 MS medium with 10 μmol/L ABA for 7 additional d. The *chl1-5* and NRT1.1$^{S585D}$/*chl1-5* seedlings grew shorter primary roots on 1/2 MS as shown above, while under ABA treatment they grew similarly to the WT and NRT1.1$^{S585A}$/*chl1-5* plants (Figure S4). These results indicated that the *chl1-5* mutant and the NRT1.1$^{S585D}$/*chl1-5* lines are slightly insensitive to ABA.

Protein phosphorylation and dephosphorylation act as molecular switches by changing enzymatic activities and/or substrate specificities, thereby regulating protein interactions, directing subcellular localization, or degrading proteins (Silva-Sanchez et al., 2015). Confocal images revealed that the NRT1.1$^{S585D}$-GFP signals were weaker than those of NRT1.1- and NRT1.1$^{S585A}$-GFP when expressed in *N. benthamiana* leaves, whereas the localization and fluorescence intensity of NRT1.1 did not differ significantly among the NRT1.1$^{S585D}$/*chl1-5*, NRT1.1$^{S585A}$/*chl1-5*, and NRT1.1/*chl1-5* transgenic lines. These results

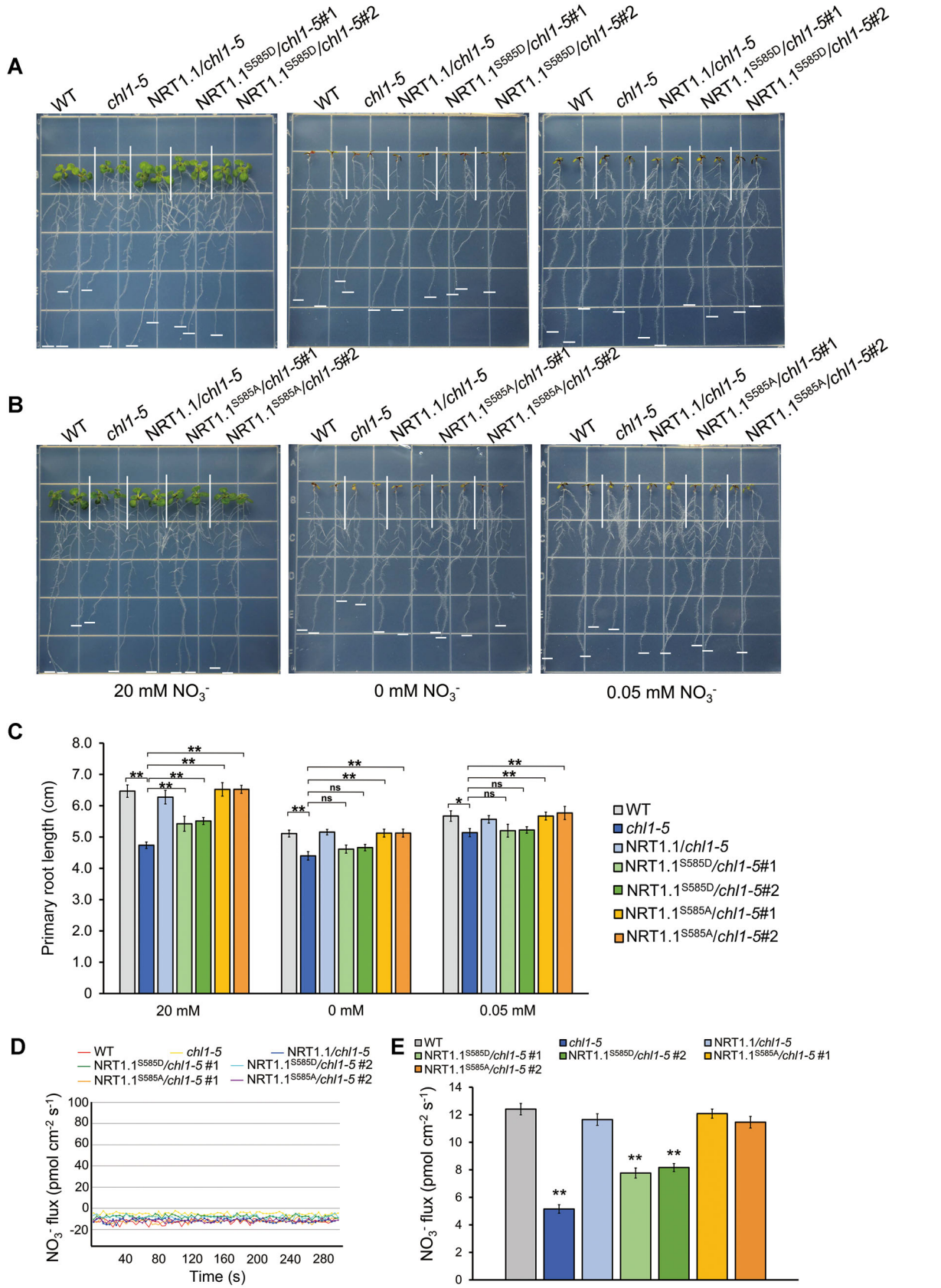


**Figure 5. Continued**

suggest that the SnRK2-mediated phosphorylation might influence transport activity, rather than localization or protein stability of NRT1.1 (Figure S6).

## DISCUSSION

The crosstalk between nitrate and plant hormones plays a vital role in plant growth and development. The provision of N can alter the biosynthesis and transport of auxin, cytokinins, and ethylene (Sakakibara et al., 2006; Tian et al., 2009; Ma et al., 2014). Recently, brassinosteroid signaling was reported to modulate the foraging of roots under low N (Jia et al., 2019). The mechanism of gibberellin crosstalk with nitrate responses improves the crop NUE immensely (Li et al., 2018). Low-nitrate conditions promote ABA accumulation (Ondzighi-Assoume et al., 2016; Lee et al., 2020). ABI2, a negative regulator of ABA signaling, enhances NRT1.1-dependent nitrate transport, sensing, and signaling. Abscisic acid has also been established to influence the expression of *NRT2/NAR*, leading to altered nitrate influx (Wang et al., 2020). However, the molecular mechanisms underlying how ABA signaling regulates nitrate deficiency still remain largely elusive.

Our results demonstrate that ABA negatively modulates the uptake of nitrate primarily through the phosphorylation of NRT1.1, indicating that ABA signaling multidimensionally modulates nitrate transport, sensing, and signaling in *Arabidopsis*. Such check and balance mechanisms likely facilitate the optimization of nitrate uptake under a limited supply of nitrate. The *aba2-1* mutant and *pyr1pyl1pyl2pyl4* and *abi1-2abi2-2hab1-1pp2ca-1* quadruple mutants exhibited a distinct root foraging phenotype, which indicated that ABA signaling is extensively involved in the regulation of the N starvation response. Furthermore, the *snrk2.2snrk2.3snrk2.6* mutant grew much longer primary roots than the WT under N deficiency, while their lateral root densities showed no difference. Since the SnRK2s have redundant functions and diverse upstream components, we hypothesized that additional SnRK2s might participate in this process (Fujii et al., 2011; Lin et al., 2020).

Although the transcriptional regulation of nitrate transport and signaling has been thoroughly investigated, the posttranslational regulation of the participants in this process is still not clear (Zhao et al., 2011; Liu et al., 2017; Kiba et al., 2018; Liu et al., 2020). As the first nitrate transporter reported to participate in nitrate uptake in higher plants and the only dual-affinity nitrate transceptor in *Arabidopsis*, NRT1.1 can be modulated to switch between the two affinities by phosphorylating threonine residue 101 (Thr101) (Ho et al., 2009). CIPK23 is the negative regulator that specifically engages in a high-affinity response by phosphorylating NRT1.1 at the Thr101 site in response to low nitrate. However, ABI2 can interact with and dephosphorylate CIPK23 and calcineurin B-like protein 1 (CBL1), leading to the inactivation of CBL1-CIPK23 complexes (Ho et al., 2009; Leran et al., 2015). An analysis of crystal structures indicated that NRT1.1 is phosphorylated by CIPK23 at Thr101 to decouple the dimer form and increase its flexibility, enabling NRT1.1 to serve as a high-affinity nitrate transporter when environmental nitrate is limited. The dephosphorylated NRT1.1 forms a dimer that has poor structural flexibility and serves as a low-affinity transporter when external nitrate is abundant (Parker and Newstead, 2014; Sun et al., 2014). Our results indicate that SnRK2.6/OST1 phosphorylate NRT1.1 at Ser585, leading to an impairment in both high- and low-affinity transport activities in oocytes. These results differ substantially from those for CIPK23, indicating that the phosphorylation of NRT1.1 by SnRK2.6/OST1 could be a novel posttranslational regulation.

NRT1.1 is a master player in the regulation of root system architecture mediated by $NO_3^-$, since it governs the growth of lateral roots depending on its auxin transport activity in response to $NO_3^-$. Previous research has dramatically illustrated that $NO_3^-$ prevents the accumulation of NRT1.1 in the lateral root primordium and the primary root tip, although $NO_3^-$ posttranscriptionally stimulates the accumulation of *NRT1.1* transcripts. These findings indicate that $NO_3^-$ promotes the accumulation of auxin in lateral root primordium and their development by two pathways, inhibiting the activity of NRT1.1 to transport auxin and preventing the accumulation of NRT1.1 protein (Bouguyon et al., 2016). This suggests that the biosynthesis and transport of auxin also regulates root foraging. Therefore, whether SnRK2s regulate the auxin transport activity of NRT1.1 merits further investigation.

In conclusion, we propose that SnRK2.2/2.3/2.6 negatively regulate the activity of NRT1.1 via phosphorylation, which alters the nitrate transport activity of NRT1.1 and root foraging under N deficiency. When nitrate is sufficient in the environment, NRT1.1 displays robust nitrate transport activity to fulfil the N demand. However, under limited N, the CBL1/9-CIPK23 complex primarily phosphorylates NRT1.1 at Thr101, promoting the transition of NRT1.1 from a low-affinity to a high-affinity nitrate transporter, thereby enhancing N absorption. Subsequently, SnRK2s primarily phosphorylate NRT1.1 at Ser585, decreasing its nitrate transport activity (Figure 6). This mechanism avoids excess nitrate absorption to balance the N stress response against the growth response.

**Figure 5. NRT1.1 phosphorylation variants regulate root growth and nitrate acquisition under nitrogen deficiency**
(**A**) Phenotypic analysis of wild type (WT), *chl1-5*, NRT1.1$^{S585D}$/*chl1-5*, and NRT1.1/*chl1-5* seedlings under 0, 0.05, and 20 mmol/L $NO_3^-$. (**B**) Phenotypic analysis of WT, *chl1-5*, NRT1.1$^{S585A}$/*chl1-5*, and NRT1.1/*chl1-5* seedlings under 0, 0.05, and 20 mmol/L $NO_3^-$. (**C**) Primary root length of the tested lines under the different nitrate treatments ($n = 24$). Error bars represent means ± *SE*. Asterisks indicate statistically significant differences according to honestly significant difference (HSD) test (*$P < 0.05$, **$P < 0.01$). (**D**) Nitrate influx rate at the root tip surface ($n = 12$). (**E**) N-influx measurement in WT, *chl1-5*, NRT1.1/*chl1-5*, NRT1.1$^{S585D}$/*chl1-5*, and NRT1.1$^{S585A}$/*chl1-5* seedlings. Error bars represent means ± *SE*. Asterisks indicate statistically significant differences according to Student's *t*-test (*$P < 0.05$, **$P < 0.01$; ns, not significant).

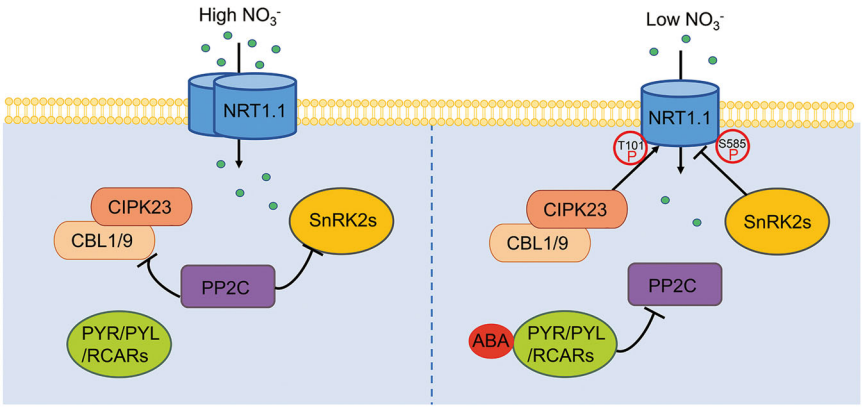


**Figure 6. Working model for the role of abscisic acid (ABA) signaling in the regulation of nitrate deficiency**
When nitrate is sufficient in the environment, NRT1.1 displays robust nitrate transport activity to fulfil the demand of the plant. When nitrate is limited, the CBL1/9-CIPK23 complex primarily phosphorylates NRT1.1 at Thr101, promoting the transition of NRT1.1 from a low-affinity to a high-affinity nitrate transporter, thereby enhancing N absorption. Subsequently, SnRK2s primarily phosphorylate NRT1.1 at Ser585, decreasing its nitrate transport activity. This mechanism avoids excess nitrate absorption to balance the N stress response against the growth response.

# MATERIALS AND METHODS

## Plant materials and growth conditions

*Arabidopsis thaliana* in the Columbia (Col-0) background was used as the WT. The *snrk2.2snrk2.3snrk2.6* triple mutant was obtained by crossing the *ost1-3* with *snrk2.2snrk2.3* lines. *SnRK2s* overexpression lines were previously described (Feng et al., 2014). To generate transgenic plants expressing NRT1.1, NRT1.1$^{S585D}$, and NRT1.1$^{S585A}$ fusions with GFP, a 1,751-bp fragment was cloned from WT *NRT1.1* cDNA and the point mutations were created by fast site-directed mutagenesis kit (TIANGEN). Then the *NRT1.1*, *NRT1.1*$^{S585D}$, and *NRT1.1*$^{S585A}$ were subcloned into a modified *pCAMBIA 1300-GFP* vector under its native promoter (~3 kb) respectively, and introduced into the *chl1-5* mutant plants by *Agrobacterium tumefaciens* GV3101.

Seeds were surface sterilized in 5% (v/v) NaClO and 0.05% (v/v) Triton X-100, then kept in darkness at 4°C for 2 d to synchronize germination. Thereafter seeds were sown on half-strength MS medium (Sigma), supplemented with 1% (w/v) sucrose, 1% (w/v) agar (Solarbio), pH 5.8, vertically placed in a growth cabinet under a 22°C/19°C and 16 h/8 h light/dark regime with light intensity adjusted to 120 μmol photons $m^{-2}$ $s^{-1}$. Homogenous 4-d-old seedlings of representative size for each genotype were transferred to nitrogen-free MS medium, supplemented with 0, 0.05, and 0.1 mmol/L $KNO_3$, sucrose and agar as described above. The primary root length of plants grown on the diverse nitrate concentrations were calculated after 7 d using Image J software.

## Nitrate content assay and flux measurement

Nitrate was measured using a salicylic acid method previously described (Xu et al., 2016). Briefly, 4-d-old seedlings germinated on 1/2 MS medium were transferred to nitrogen-free MS medium, supplemented with 0.05 mmol/L $KNO_3$. After another 4 d treatment, roots of these plants were transferred to measuring solution. The nitrate fluxes were measured using a high-resolution scanning ion-selective electrode technique (NMT150; Younger USA Science and Technology Corp). The method was previously described in detail (He et al., 2015).

## Yeast two-hybrid assay

For split-ubiquitin analysis, the DUAL membrane kit3 (Dualsystems Biotech) was used. The full-length cDNAs of interest were cloned in frame with either the C-terminal (Cub) or N-terminal (Nub) subdomain of ubiquitin, then introduced into yeast strain NMY51 by the lithium acetate method.

## Transient assay in *N. benthamiana*

Bimolecular fluorescence complementation experiments were performed in transiently transformed *N. benthamiana* leaves of 4- to 5-week-old plants. The full-length cDNAs of interest were cloned into the *SPYCE* (*M*) and *SPYNE* (*R*) vector. For coinfiltration experiments, equal volumes of an *Agrobacterium tumefaciens* (strain EHA105) culture containing *35 S:SnRK2s-SPYNE* and *35 S:NRT1.1-SPYCE* ($OD_{600}$ = 1.5) were mixed before infiltration into *N. benthamiana* leaves. Fluorescent microscopy of abaxial leaf epidermal cells was performed 3 d after infiltration using Confocal Laser Scanning Microscope Olympus IX83-FV3000.

The luciferase complementation imaging assays were carried out briefly as follows. The *Agrobacterium tumefaciens* (strain GV3101)-mediated transformation was performed as mentioned before. After infiltration, plants were cultured at 23°C for 48 h at 16 h (light)–8 h (dark) photoperiod. The infiltrated leaves were sprayed with 1 mmol/L luciferin (Sigma) in darkness for 10 min before detection of luminescence. Images of luminescence were captured by a low-light-cooled charge-coupled device imaging apparatus (Lumazone Pylon 2048B; Princeton).

### Co-immunoprecipitation assay

The coding sequence of SnRK2.6/OST1 was cloned into the *pCAMBIA1300-6myc* vector and coding sequence of NRT1.1 N and NRT1.1 C were cloned into *pCAMBIA1300-eGFP* vector. Total protein was extracted from infiltrated tobacco leaves with protein extraction buffer (50 mmol/L Tris-MES (2-[*N*-morpholino]ethanesulfonic acid) (pH8.0), 0.5 mol/L sucrose, 1 mmol/L $MgCl_2$, 10 mmol/L ethylenediaminetetraacetic acid, 5 mmol/L dithiothreitol (DTT), 1× protease inhibitor cocktail and 0.1% NP-40). Then, supernatant was incubated with polyclonal anti-MYC (Abmart) overnight at 4°C with gentle shaking. The immune complexes were incubated with anti-MYC agarose beads for 2 h at 4°C and were washed three times with extraction buffer. The precipitated proteins were eluted with 2× SDS loading buffer at 95°C for 5 min. Then, the immunoprecipitation products were detected by immunoblot analysis.

### Protein kinase assay

*In vitro* phosphorylation and in-gel kinase assays were performed as described (Ding et al., 2015). The coding sequence of *SnRK2.6/OST1* was cloned into *pMAL-c2X* vector and the coding sequence of *NRT1.1* was cloned into *pGEX-4T-1* vector. Recombinant plasmids were transformed into *E. coli* BL21 and recombinant proteins were purified separately. First, a 20 μL kinase solution containing 20 mmol/L Tris-HCl (pH 7.5), 20 mmol/L $MgCl_2$, 1 mmol/L DTT, 1 μg SnRK2.6/OST1 kinase protein and 3 μg NRT1.1 protein was prepared. Then, phosphorylation was initiated by adding 1.1 μL Ci [$\gamma$-$^{32}$P] ATP. After incubation for 30 min at 30°C, reactions were stopped by adding 5 μL 5× loading buffer and boiling for 5 min. Through SDS-PAGE of the reaction products, the phosphorylated proteins were visualized by autoradiography.

For in-gel kinase assay, total protein prepared from 10 d WT and *snrk2.2snrk2.3snrk2.6* plants with or without 50 μmol/L ABA were separated by SDS-PAGE gel containing 0.1 mg/mL GST-NRT1.1 substrate. After washing by washing solution (1 mmol/L DTT, 5 mmol/L NaF, 0.1 mmol/L $Na_3VO_4$, 0.5 mg/mL bovine serum albumin (BSA), 0.1% Triton X-100, and 25 mmol/L Tris–HCl, pH 7.5) three times, the gel was renatured by buffer (2 mmol/L DTT, 5 mmol/L NaF, 0.1 mmol/L $Na_3VO_4$, and 25 mmol/L Tris-HCl, pH 7.5). Through kinase reaction with [$\gamma$-$^{32}$P], the signals were visualized by autoradiography.

### $^{15}NO_3^-$ uptake assay in *Xenopus* oocytes

$^{15}NO_3^-$ uptake assay was performed as described (Ho et al., 2009) with slight modification. For expression in *Xenopus* oocytes, the full-length cDNA of *NRT1.1* and *SnRK2.6/OST1* were cloned into the vector *pNB1*. The RiboMAX™ Large Scale RNA Production System-T7 (Promega) was used for cRNA synthesizing. The oocytes were injected with distilled water (50 nL as control) and experimental group (50 nL) the concentration of which was adjusted to 1,000 ng/μL. After incubation in ND96 medium (96 mmol/L NaCl, 1 mmol/L $MgCl_2$, 1 mmol/L $CaCl_2$, 10 mmol/L MES, adjusted to pH 7.5 with Tris-base) for 2 d at 16°C, oocytes were treated for 4 h in ND96 medium (pH 7.4) containing 10 or 0.5 mmol/L $^{15}$N-nitrate (atom % $^{15}$N abundance, 99.9%). Oocytes were then washed five times using ND96 medium. After being completely dried at 65°C, batches of 8–10 oocytes were then analyzed for total nitrogen content and atom % $^{15}$N abundance by continuous-flow mass spectrometry (ANCA-GSL MS; PDZ Europa).

### Statistical analysis

Data are given as means ± *SE* of one representative experiment with $n \geq 4$ individual plants. Each experiment was repeated independently at least two times with similar results. The significance between the means of different treatments/genotypes was evaluated by Student's *t*-tests and Tukey's honestly significant difference (HSD) tests using SPSS version 19.0 software (IBM).

## ACKNOWLEDGEMENTS

We thank Dr. Zhizhong Gong (China Agricultural University) for technical assistance, and Dr. Hua Zhao and Dr. Fengping Yuan (State Key Laboratory of Crop Stress Biology for Arid Areas, Northwest A&F University, Yangling, China) for confocal experimental assistance. This research was funded by a grant from the Northwest A&F University (Z111021604 to C.W.), the National Natural Science Foundation of China (31770289 to C.W.), Natural Science Basic Research Plan in Shaanxi Province of China (2019JQ-135 to C.W.), and the Opening Research Projects of National Key Laboratory of Plant Molecular Genetics, CEMPS, CAS.

## AUTHOR CONTRIBUTIONS

C.W., and H.T. designed the study. H.S., T.W., C.J., J.D., T.Z., M.L., and H.T. performed the experiments. H.S. and C. W. analyzed the data and wrote the manuscript. All authors read and approved of the manuscript.

**Edited by:** Pengcheng Wang, Shanghai Center for Plant Stress Biology, CAS, China

**Received** Sep. 23, 2020; **Accepted** Dec. 14, 2020; **Published** Dec. 17, 2020

## REFERENCES

**Bouguyon, E., Brun, F., Meynard, D., Kubes, M., Pervent, M., Leran, S., Lacombe, B., Krouk, G., Guiderdoni, E., Zazimalova, E., Hoyerova, K., Nacry, P., and Gojon, A.** (2015). Multiple mechanisms of nitrate sensing by *Arabidopsis* nitrate transceptor NRT1.1. Nat. Plants **1:** 15015.

**Bouguyon, E., Perrine-Walker, F., Pervent, M., Rochette, J., Cuesta, C., Benkova, E., Martiniere, A., Bach, L., Krouk, G., Gojon, A., and Nacry, P.** (2016). Nitrate controls root development through

posttranscriptional regulation of the NRT1.1/NPF6.3 transporter/sensor. Plant Physiol. **172:** 1237–1248.

**Chen, K., Li, G.J., Ray, A.B., Song, C.P., and Zhao, Y.** (2020). Abscisic acid dynamics, signaling, and functions in plants. J. Integr. Plant Biol. **62:** 25–54.

**Ding, Y., Li, H., Zhang, X., Xie, Q., Gong, Z., and Yang, S.** (2015). OST1 kinase modulates freezing tolerance by enhancing ICE1 stability in *Arabidopsis*. Dev. Cell **32:** 278–289.

**Feng, C.Z., Chen, Y., Wang, C., Kong, Y.H., Wu, W.H., and Chen, Y.F.** (2014). *Arabidopsis* RAV1 transcription factor, phosphorylated by SnRK2 kinases, regulates the expression of ABI3, ABI4, and ABI5 during seed germination and early seedling development. Plant J. **80:** 654–668.

**Fujii, H., Verslues, P.E., and Zhu, J.K.** (2011). *Arabidopsis* decuple mutant reveals the importance of SnRK2 kinases in osmotic stress responses *in vivo*. Proc. Natl. Acad. Sci. USA **108:** 1717–1722.

**Fujii, H., and Zhu, J.K.** (2009). *Arabidopsis* mutant deficient in 3 abscisic acid-activated protein kinases reveals critical roles in growth, reproduction, and stress. Proc. Natl. Acad. Sci. USA **106:** 8380–8385.

**Fujita, Y., Nakashima, K., Yoshida, T., Katagiri, T., Kidokoro, S., Kanamori, N., Umezawa, T., Fujita, M., Maruyama, K., Ishiyama, K., Kobayashi, M., Nakasone, S., Yamada, K., Ito, T., Shinozaki, K., and Yamaguchi-Shinozaki, K.** (2009). Three SnRK2 protein kinases are the main positive regulators of abscisic acid signaling in response to water stress in *Arabidopsis*. Plant Cell Physiol. **50:** 2123–2132.

**Geiger, D., Scherzer, S., Mumm, P., Stange, A., Marten, I., Bauer, H., Ache, P., Matschi, S., Liese, A., Al-Rasheid, K.A., Romeis, T., and Hedrich, R.** (2009). Activity of guard cell anion channel SLAC1 is controlled by drought-stress signaling kinase-phosphatase pair. Proc. Natl. Acad. Sci. USA **106:** 21425–21430.

**Giehl, R.F.H., and Wiren, N.V.** (2014). Root nutrient foraging. Plant Physiol. **166:** 509–517.

**Gonzalez-Guzman, M., Pizzio, G.A., Antoni, R., Vera-Sirera, F., Merilo, E., Bassel, G.W., Fernandez, M.A., Holdsworth, M.J., Perez-Amador, M.A., Kollist, H., and Rodriguez, P.L.** (2012). *Arabidopsis* PYR/PYL/RCAR receptors play a major role in quantitative regulation of stomatal aperture and transcriptional response to abscisic acid. Plant Cell **24:** 2483–2496.

**Gruber, B.D., Giehl, R.F.H., Friedel, S., and Wiren, N.V.** (2013). Plasticity of the *Arabidopsis* root system under nutrient deficiencies. Plant Physiol. **163:** 161–179.

**Guan, P., Wang, R., Nacry, P., Breton, G., Kay, S.A., Pruneda-Paz, J.L., Davani, A., and Crawford, N.M.** (2014). Nitrate foraging by *Arabidopsis* roots is mediated by the transcription factor TCP20 through the systemic signaling pathway. Proc. Natl. Acad. Sci. USA **111:** 15267–15272.

**He, X., Qu, B., Li, W., Zhao, X., Teng, W., Ma, W., Ren, Y., Li, B., Li, Z., and Tong, Y.** (2015). The nitrate-inducible NAC transcription factor TaNAC2-5A controls nitrate response and increases wheat yield. Plant Physiol. **169:** 1991–2005.

**Ho, C.H., Lin, S.H., Hu, H.C., and Tsay, Y.F.** (2009). CHL1 functions as a nitrate sensor in plants. Cell **138:** 1184–1194.

**Huang, N.C., Chiang, S.C., Crawford, N.M., and Tsay, Y.F.** (1996). CHL1 encodes a component of the low-affinity nitrate uptake system in *Arabidopsis* and shows cell type-specific expression in roots. Plant Cell **8:** 2183–2191.

**Jia, Z., Giehl, R.F.H., Meyer, R.C., Altmann, T., and Wiren, N.V.** (2019). Natural variation of BSK3 tunes brassinosteroid signaling to regulate root foraging under low nitrogen. Nat. Commun. **10:** 2378.

**Kiba, T., Feria-Bourrellier, A.B., Lafouge, F., Lezhneva, L., Boutet-Mercey, S., Orsel, M., Brehaut, V., Miller, A., Daniel-Vedele, F., Sakakibara, H., and Krapp, A.** (2012). The *Arabidopsis* nitrate transporter NRT2.4 plays a double role in roots and shoots of nitrogen-starved plants. Plant Cell **24:** 245–258.

**Kiba, T., Inaba, J., Kudo, T., Ueda, N., Konishi, M., Mitsuda, N., Takiguchi, Y., Kondou, Y., Yoshizumi, T., Ohme-Takagi, M., Matsui, M., Yano, K., Yanagisawa, S., and Sakakibara, H.** (2018). Repression of nitrogen starvation responses by members of the *Arabidopsis* GARP-type transcription factor NIGT1/HRS1 subfamily. Plant Cell **30:** 925–945.

**Krouk, G., Lacombe, B., Bielach, A., Perrine-Walker, F., Malinska, K., Mounier, E., Hoyerova, K., Tillard, P., Leon, S., Ljung, K., Zazimalova, E., Benkova, E., Nacry, P., and Gojon, A.** (2010). Nitrate-regulated auxin transport by NRT1.1 defines a mechanism for nutrient sensing in plants. Dev. Cell **18:** 927–937.

**Lee, H.G., and Seo, P.J.** (2019). MYB96 recruits the HDA15 protein to suppress negative regulators of ABA signaling in *Arabidopsis*. Nat. Commun. **10:** 1713.

**Lee, W.J., Truong, H.A., Trinh, C.S., Kim, J.H., Lee, S., Hong, S.W., and Lee, H.** (2020). *NITROGEN RESPONSE DEFICIENCY1*-mediated *CHL1* induction contributes to optimized growth performance during altered nitrate availability in *Arabidopsis*. Plant J. **104**(5): 1382–1398.

**Leran, S., Edel, K.H., Pervent, M., Hashimoto, K., Corratge-Faillie, C., Offenborn, J.N., Tillard, P., Gojon, A., Kudla, J., and Lacombe, B.** (2015). Nitrate sensing and uptake in *Arabidopsis* are enhanced by ABI2, a phosphatase inactivated by the stress hormone abscisic acid. Sci. Signal. **8:** 375.

**Leran, S., Munos, S., Brachet, C., Tillard, P., Gojon, A., and Lacombe, B.** (2013). *Arabidopsis* NRT1.1 is a bidirectional transporter involved in root-to-shoot nitrate translocation. Mol. Plant **6:** 1984–1987.

**Lezhneva, L., Kiba, T., Feria-Bourrellier, A.B., Lafouge, F., Boutet-Mercey, S., Zoufan, P., Sakakibara, H., Daniel-Vedele, F., and Krapp, A.** (2014). The *Arabidopsis* nitrate transporter NRT2.5 plays a role in nitrate acquisition and remobilization in nitrogen-starved plants. Plant J. **80:** 230–241.

**Li, S., Tian, Y., Wu, K., Ye, Y., Yu, J., Zhang, J., Liu, Q., Hu, M., Li, H., Tong, Y., Harberd, N.P., and Fu, X.** (2018). Modulating plant growth-metabolism coordination for sustainable agriculture. Nature **560:** 595–600.

**Li, W., Wang, Y., Okamoto, M., Crawford, N.M., Siddiqi, M.Y., and Glass, A.D.** (2007). Dissection of the AtNRT2.1: AtNRT2.2 inducible high-affinity nitrate transporter gene cluster. Plant Physiol. **143:** 425–433.

**Lin, Y.L., and Tsay, Y.F.** (2017). Influence of differing nitrate and nitrogen availability on flowering control in *Arabidopsis*. J. Exp. Bot. **68:** 2603–2609.

**Lin, Z., Li, Y., Zhang, Z.J., Liu, X.L., Hsu, C.C., Du, Y.Y., Sang, T., Zhu, C., Wang, Y.B., Satheesh, V., Pratibha, P., Zhao, Y., Song, C.P., Tao, W.A., Zhu, J.K., and Wang, P.C.** (2020). A RAF-SnRK2 kinase cascade mediates early osmotic stress signaling in higher plants. Nat. Commun. **11:** 613.

**Liu, K.H., Diener, A., Lin, Z.W., Liu, C., and Sheen, J.** (2020). Primary nitrate responses via calcium signalling and diverse protein phosphorylation. J. Exp. Bot. **71:** 4428–4441.

**Liu, K.H., Niu, Y., Konishi, M., Wu, Y., Du, H., Sun, C.H., Li, L., Boudsocq, M., McCormack, M., Maekawa, S., Ishida, T., Zhang, C., Shokat, K., Yanagisawa, S., and Sheen, J.** (2017). Discovery of nitrate-CPK-NLP signalling in central nutrient-growth networks. Nature **545:** 311–316.

**Liu, K.H., and Tsay, Y.F.** (2003). Switching between the two action modes of the dual-affinity nitrate transporter CHL1 by phosphorylation. EMBO J. **22:** 1005–1013.

**Ma, W., Li, J., Qu, B., He, X., Zhao, X., Li, B., Fu, X., and Tong, Y.** (2014). Auxin biosynthetic gene *TAR2* is involved in low nitrogen-mediated reprogramming of root architecture in *Arabidopsis*. Plant J. **78:** 70–79.

**Mergner, J., Frejno, M., List, M., Papacek, M., Chen, X., Chaudhary, A., Samaras, P., Richter, S., Shikata, H., Messerer, M., Lang, D., Altmann, S., Cyprys, P., Zolg, D.P., Mathieson, T., Bantscheff, M., Hazarika, R.R., Schmidt, T., Dawid, C., Dunkel, A., Hofmann, T., Sprunck, S., Falter-Braun, P., Johannes, F., Mayer, K.F.X., Jurgens,**

**G., Wilhelm, M., Baumbach, J., Grill, E., Schneitz, K., Schwechheimer, C., and Kuster, B.** (2020). Mass-spectrometry-based draft of the *Arabidopsis* proteome. Nature **579:** 409–414.

**Miller, A.J., and Cramer, M.D.** (2004). Root nitrogen acquisition and assimilation. Plant Soil **4:** 1–36.

**Nuruzzaman, M., Sharoni, A.M., and Kikuchi, S.** (2013). Roles of NAC transcription factors in the regulation of biotic and abiotic stress responses in plants. Front. Microbiol. **4:** 248.

**O'Brien, J.A., Vega, A., Bouguyon, E., Krouk, G., Gojon, A., Coruzzi, G., and Gutierrez, R.A.** (2016). Nitrate transport, sensing, and responses in plants. Mol. Plant **9:** 837–856.

**Ohkubo, Y., Tanaka, M., Tabata, R., Ogawa-Ohnishi, M., and Matsubayashi, Y.** (2017). Shoot-to-root mobile polypeptides involved in systemic regulation of nitrogen acquisition. Nat. Plants **3:** 17029.

**Oldroyd, G.E.D., and Leyser, O.** (2020). A plant's diet, surviving in a variable nutrient environment. Science **368:** 45.

**Ondzighi-Assoume, C.A., Chakraborty, S., and Harris, J.M.** (2016). Environmental nitrate stimulates abscisic acid accumulation in arabidopsis root tips by releasing it from inactive stores. Plant Cell **28:** 729–745.

**Osugi, A., Kojima, M., Takebayashi, Y., Ueda, N., Kiba, T., and Sakakibara, H.** (2017). Systemic transport of trans-zeatin and its precursor have differing roles in *Arabidopsis* shoots. Nat. Plants **3:** 17112.

**Parker, J.L., and Newstead, S.** (2014). Molecular basis of nitrate uptake by the plant nitrate transporter NRT1.1. Nature **507:** 68–72.

**Qi, L., Liu, S., Li, C., Fu, J., Jing, Y., Cheng, J., Li, H., Zhang, D., Wang, X., Dong, X., Han, R., Li, B., Zhang, Y., Li, Z., Terzaghi, W., Song, C.P., Lin, R., Gong, Z., and Li, J.** (2020). PHYTOCHROME-INTERACTING FACTORS interact with the ABA receptors PYL8 and PYL9 to orchestrate ABA signaling in darkness. Mol. Plant **13:** 414–430.

**Rubin, G., Tohge, T., Matsuda, F., Saito, K., and Scheible, W.R.** (2009). Members of the LBD family of transcription factors repress anthocyanin synthesis and affect additional nitrogen responses in *Arabidopsis*. Plant Cell **21:** 3567–3584.

**Sakakibara, H., Takei, K., and Hirose, N.** (2006). Interactions between nitrogen and cytokinin in the regulation of metabolism and development. Trends Plant Sci. **11:** 440–448.

**Sato, A., Sato, Y., Fukao, Y., Fujiwara, M., Umezawa, T., Shinozaki, K., Hibi, T., Taniguchi, M., Miyake, H., Goto, D.B., and Uozumi, N.** (2009). Threonine at position 306 of the KAT1 potassium channel is essential for channel activity and is a target site for ABA-activated SnRK2/OST1/SnRK2.6 protein kinase. Biochem. J. **424:** 439–448.

**Silva-Sanchez, C., Li, H., and Chen, S.** (2015). Recent advances and challenges in plant phosphoproteomics. Proteomics **15:** 1127–1141.

**Sirichandra, C., Gu, D., Hu, H.C., Davanture, M., Lee, S., Djaoui, M., Valot, B., Zivy, M., Leung, J., Merlot, S., and Kwak, J.M.** (2009). Phosphorylation of the *Arabidopsis* AtrbohF NADPH oxidase by OST1 protein kinase. FEBS Lett. **583:** 2982–2986.

**Sun, J., Bankston, J.R., Payandeh, J., Hinds, T.R., Zagotta, W.N., and Zheng, N.** (2014). Crystal structure of the plant dual-affinity nitrate transporter NRT1.1. Nature **507:** 73–77.

**Tian, Q.Y., Sun, P., and Zhang, W.H.** (2009). Ethylene is involved in nitrate-dependent root growth and branching in *Arabidopsis thaliana*. New Phytol. **184:** 918–931.

**Tsay, Y.F., Schroeder, J.I., Feldmann, K.A., and Crawford, N.M.** (1993). The herbicide sensitivity gene CHL1 of *Arabidopsis* encodes a nitrate-inducible nitrate transporter. Cell **72:** 705–713.

**Umezawa, T., Sugiyama, N., Mizoguchi, M., Hayashi, S., Myouga, F., Yamaguchi-Shinozaki, K., Ishihama, Y., Hirayama, T., and Shinozaki, K.** (2009). Type 2C protein phosphatases directly regulate abscisic acid-activated protein kinases in *Arabidopsis*. Proc. Natl. Acad. Sci. USA **106:** 17588–17593.

**Wang, M., Zhang, P., Liu, Q., Li, G., Di, D., Xia, G., Kronzucker, H., Fang, S., Chu, J., and Shi, W.M.** (2020). TaANR1-TaBG1 and TaWabi5-TaNRT2s/NARs link ABA metabolism and nitrate acquisition in wheat roots. Plant Physiol. **182**(3): 1440–1453.

**Wang, Y.Y., Cheng, Y.H., Chen, K.E., and Tsay, Y.F.** (2018). Nitrate transport, signaling, and use efficiency. Annu. Rev. Plant Biol. **69:** 85–122.

**Xu, N., Wang, R., Zhao, L., Zhang, C., Li, Z., Lei, Z., Liu, F., Guan, P., Chu, Z., Crawford, N.M., and Wang, Y.** (2016). The *Arabidopsis* NRG2 protein mediates nitrate signaling and interacts with and regulates key nitrate regulators. Plant Cell **28:** 485–504.

**Xu, X., Wan, W., Jiang, G., Xi, Y., Huang, H., Cai, J., Chang, Y., Duan, C. G., Mangrauthia, S.K., Peng, X., Zhu, J.K., and Zhu, G.** (2019). Nucleocytoplasmic trafficking of the *Arabidopsis* WD40 repeat protein XIW1 regulates ABI5 stability and abscisic acid responses. Mol. Plant **12:** 1598–1611.

**Zhang, X., Cui, Y., Yu, M., Su, B., Gong, W., Baluska, F., Komis, G., Samaj, J., Shan, X., and Lin, J.** (2019). Phosphorylation-mediated dynamics of nitrate transceptor NRT1.1 regulate auxin flux and nitrate signaling in lateral root growth. Plant Physiol. **181:** 480–498.

**Zhao, M., Ding, H., Zhu, J.K., Zhang, F., and Li, W.X.** (2011). Involvement of miR169 in the nitrogen-starvation responses in *Arabidopsis*. New Phytol. **190:** 906–915.

## SUPPORTING INFORMATION

Additional Supporting Information may be found online in the supporting information tab for this article: http://onlinelibrary.wiley.com/doi/10.1111/jipb.13057/suppinfo

**Figure S1.** Phenotypic analysis of the *snrk2* single and double mutants under nitrogen deficiency

(**A**) Phenotype of the *snrk2.6* mutant under 0, 0.05, and 20 mmol/L $NO_3^-$. (**B**) Primary root length of the *snrk2.6* mutant under the different nitrate treatments ($n = 24$). (**C**) Phenotype of the *snrk2.2snrk2.3* double mutant under 0, 0.05, and 20 mmol/L $NO_3^-$. (**D**) Primary root length of the *snrk2.2snrk2.3* mutant under the different nitrate treatments ($n = 24$). Error bars represent means ± *SE*. Asterisks indicate statistically significant differences according to honestly significant difference (HSD) test ($^*P < 0.05$).

**Figure S2.** Phenotypic analysis of the *SnRK2* overexpression lines under nitrogen deficiency

(**A**) Phenotypes of the *SnRK2.2*, *SnRK2.3*, and *SnRK2.6/OST1* overexpression lines under 0, 0.05, and 20 mmol/L $NO_3^-$. (**B**) Primary root length of these lines under the different nitrate treatments ($n = 24$). (**C**) Lateral root density under the different treatments ($n = 24$). Error bars represent means ± *SE*. Asterisks indicate statistically significant differences according to honestly significant difference (HSD) test ($^*P < 0.05$).

**Figure S3.** Phenotypic analysis of NRT1.1 phosphorylation variants under nitrogen deficiency

(**A**) Phenotypic analysis of wild type (WT), *chl1-5*, NRT1.1$^{S8D}$/*chl1-5*, and NRT1.1/*chl1-5* seedlings under 0, 0.05, and 20 mmol/L $NO_3^-$. (**B**) Phenotypic analysis of WT, *chl1-5*, NRT1.1$^{S8A}$/*chl1-5*, and NRT1.1/*chl1-5* seedlings under 0, 0.05, and 20 mmol/L $NO_3^-$. (**C**) Primary root length of the tested lines under the different nitrate treatments ($n = 24$). Error bars represent means ± *SE*. Asterisks indicate statistically significant differences according to honestly significant difference (HSD) test ($^*P < 0.05$, $^{**}P < 0.01$).

**Figure S4.** Phenotypic analysis of NRT1.1 phosphorylation variants with abscisic acid (ABA) treatment

(**A**) Phenotypic analysis of wild type (WT), *chl1-5*, NRT1.1$^{S585D}$/*chl1-5*, NRT1.1$^{S58AD}$/*chl1-5*, and NRT1.1/*chl1-5* seedlings treated with 10 μmol/L ABA. (**B**) Primary root length of the tested lines with and without 10 μmol/L ABA ($n = 24$). Error bars represent means ± *SE*. Asterisks indicate statistically significant differences according to honestly significant difference (HSD) test ($^{**}P < 0.01$).

**Figure S5**. Identification of the expression level of *NRT1.1*

Reverse transcription polymerase chain reaction analysis of *NRT1.1* expression in wild type (WT), *chl1-5*, NRT1.1/*chl1-5*, NRT1.1$^{S585D}$/*chl1-5*, NRT1.1$^{S585A}$/*chl1-5*, NRT1.1$^{S8D}$/*chl1-5*, and NRT1.1$^{S8A}$/*chl1-5* seedlings. *Actin* was used as the internal control.

**Figure S6.** Localization and protein stability of NRT1.1-GFP, NRT1.1$^{S585D}$-GFP, and NRT1.1$^{S585A}$-GFP

(**A**) Confocal images of NRT1.1-GFP, NRT1.1$^{S585D}$-GFP, and NRT1.1$^{S585A}$-GFP expressed in *Nicotiana benthamiana* leaves. Scale bar = 30 μm. (**B**) The roots of transgenic NRT1.1-GFP, NRT1.1$^{S585D}$-GFP, and NRT1.1$^{S585A}$-GFP plants. Roots were stained with propidium iodide and imaged with a laser-scanning confocal microscope using 561 nm and 650–710 nm. Green fluorescent protein (GFP) was excited with a 488 nm laser and emission was detected between 505 and 530 nm. Scale bar = 50 μm.